Department of Physics and Astronomy
Vanderbilt University
Nashville, Tennessee 37203

Nuclear Pumped Laser II

Final Report

August 1975 - August 1977

NASA Grant Number NSG 1232

by

Russell J. DeYoung
Ja H. Lee, Principal Investigator
W. T. Pinkston

Dr. Frank Hohl
The NASA Technical Officer for the Grant
NASA Langley Research Center
Hampton, VA 23665

VU-PL 7/77

TABLE OF CONTENTS

ABSTRACT

This final report describes the accomplishments achieved under NASA Grant NSG-1232. The first direct nuclear-pumped laser using the $^{3}He(n,p)^{3}H$ reaction was developed during the grant period. Lasing took place on the 1.79μ Ar I transition in a mixture of ^{3}He-Ar at approximately 600 Torr total pressure. It was found that the electrically pulsed afterglow He-Ar laser had the same concentration profile as the nuclear-pumped laser. Thus, electrical afterglow lasers could be used to optimize potential nuclear lasers. As a result, nuclear lasing was also achieved in ^{3}He-Xe (2.027μ) and ^{3}He-Kr (2.52μ). Scaling of laser output with both thermal flux and total pressure as well as minority concentration has been completed. A peak output (^{3}He-Ar) of 3.7 watts has been achieved at a total pressure of 4 atm. Direct nuclear pumping of ^{3}He-Ne has also been achieved, although the wavelength is not known as yet. Nuclear pumping of a ^{3}He-NF_3 mixture was attempted, lasing in FI at ∿7000 Å, without success, although the potential lasing transitions appeared in spontaneous emission. Both NF_3 and $^{238}UF_6$ appear to quench spontaneous emission when they constitute more than 1% of the gas mixture.

INTRODUCTION

This final report under NASA Grant NSG-1232 will summarize the research accomplished during the grant period August 1975 to August 1977. Figure 1 shows a block diagram of the research carried out during the grant period. Research results associated within each block will be discussed below.

BASIC LASER AND GASEOUS ELECTRONICS RESEARCH

Laser research at the reactor site is very difficult and costly. Thus, as much knowledge as possible must be gained in the laboratory before going to the reactor site. Heavy emphasis has thus been placed on electrically-pulsed afterglow lasers which can easily be studied in the laboratory environment.

Two separate high-vacuum systems were constructed along with two electrical pulse modulators which could deliver 60 kV at 100 amps in a 0.5 μsec electrical pulse to the laser cell. The vacuum systems were capable of 10^{-6} Torr and research grade gases were used in all laboratory experiments.

In the work of J. Guyot,[1] it was demonstrated that large concentrations of helium metastables could be generated in the reactor using a boron-10 coated tube to excite (α-particles) the helium gas. This stored energy (helium metastables) could then be transferred to a minority gas species which would then lase. Thus, laboratory experiments were constructed to demonstrate that high concentrations of helium metastables could also be produced in the electrically-pulsed afterglow at high pressures and thus, this method could be used to study the reactor (charged particle) produced plasma. Figure 2 shows the results of these experiments. The 3889Å He-line was used to probe the $He(2^3S)$ density while the 5016Å He-line probed the $He(2^1S)$ density. Absorption measurements were taken 56 μsec after the termination of the electrical pulse, therefore, we are definitely probing the afterglow

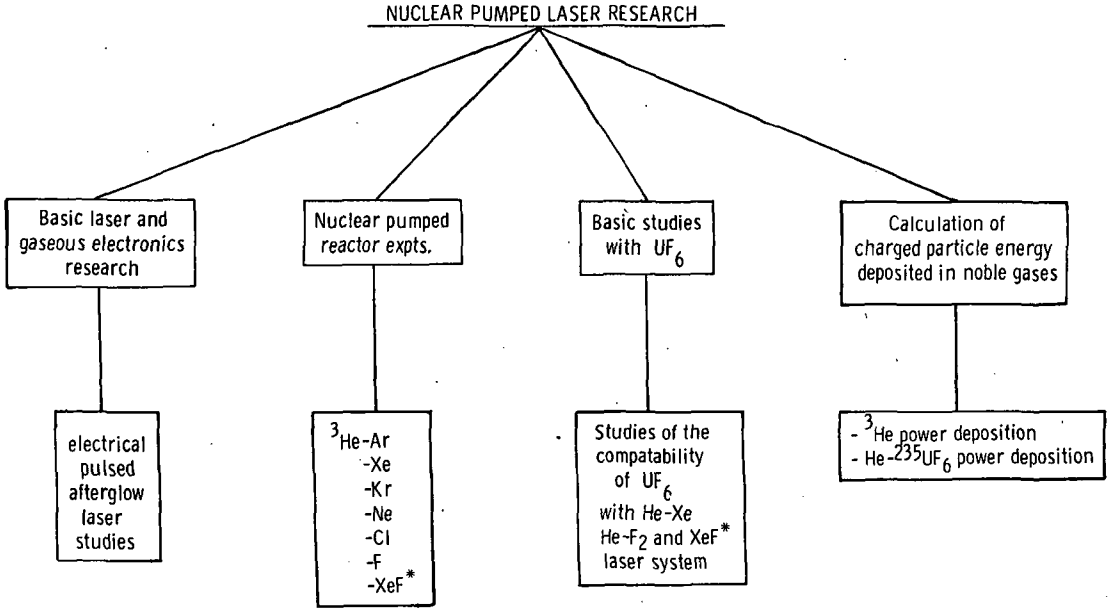
NUCLEAR PUMPED LASER RESEARCH
Basic laser and gaseous electronics research
Nuclear pumped reactor expts.
Basic studies with UF_6
Calculation of charged particle energy deposited in noble gases
electrical pulsed afterglow laser studies
^{3}He-Ar
-Xe
-Kr
-Ne
-Cl
-F
-XeF*
Studies of the compatability of UF_6 with He-Xe He-F_2 and XeF* laser system
- ^{3}He power deposition
- He-$^{235}UF_6$ power deposition

Fig. 1

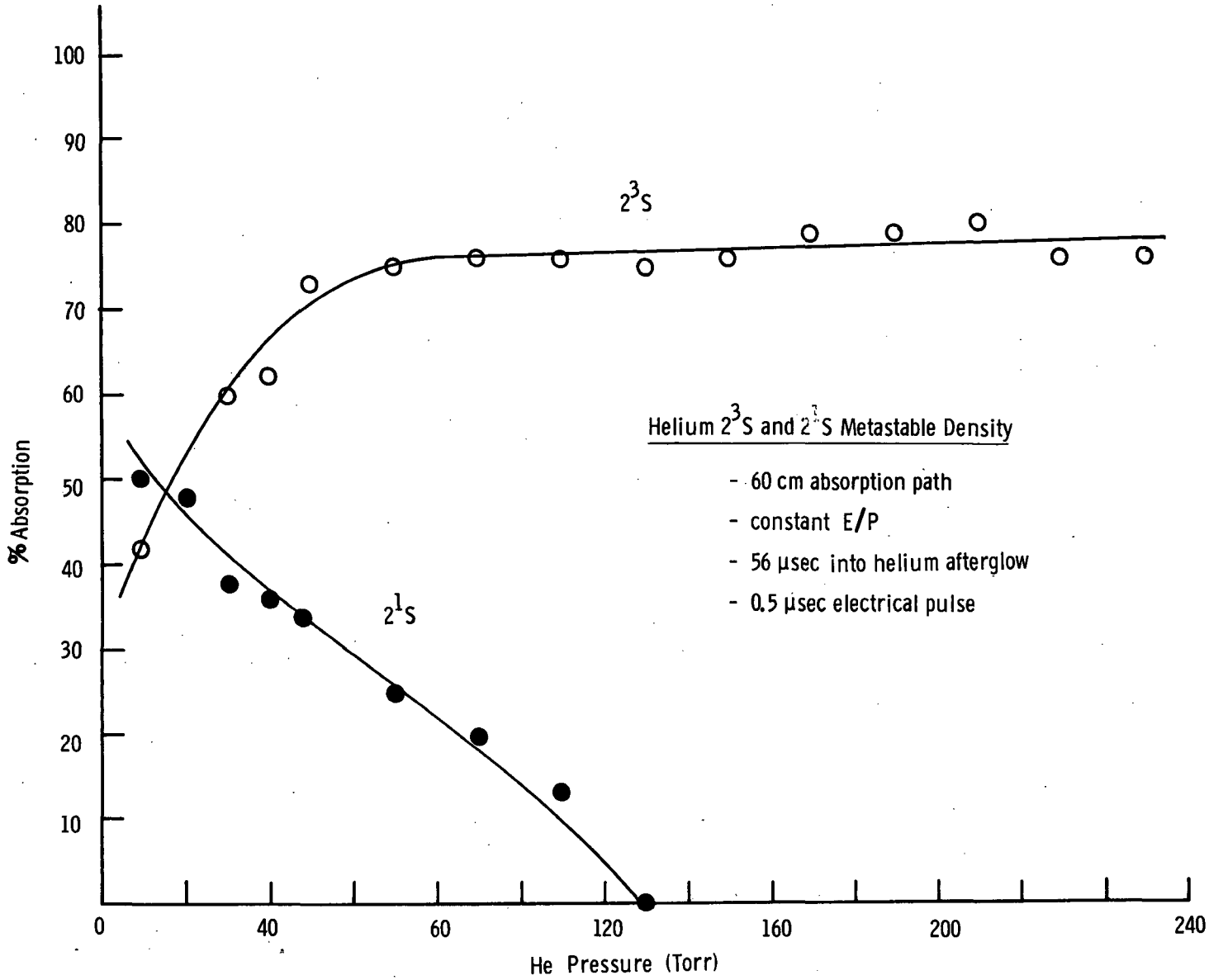
100
90
80
70
60
50
40
30
20
10
% Absorption
2^3S
2^1S
Helium 2^3S and 2^1S Metastable Density
- 60 cm absorption path
- constant E/P
- 56 µsec into helium afterglow
- 0.5 µsec electrical pulse
0
40
60
120
160
200
240
He Pressure (Torr)

Fig. 2

plasma. Note that with increasing pressure, the 2^1S metastables rapidly convert into 2^3S metastables. From the measurements, it can be concluded that sufficient densities of helium metastables exist late in the afterglow, and these long-lived states might transfer their stored energy to a minority species.

Dielectric laser mirrors were then placed at the ends of the discharge tube and lasing was achieved in all the noble gases (except He) at various wavelengths. Figure 3 shows typical results of lasing under the present laboratory experimental setup. Note that there are two distinct laser pulses. The first laser output appears during the voltage pulse and this most probably corresponds to direct electron impact excitation of the upper laser level. The second pulse occurs in the afterglow period and is much longer in duration than the first laser pulse. This secondary laser pulse, as discussed later, probably corresponds to Penning ionization of the minority gas species by the He metastables followed by collisional radiative recombination of the atomic ion and then radiative decay into the upper laser level. These same results were found for He-Ar, He-Kr, and He-Ne. Not all transitions that lased, lased in the afterglow. Some transitions only lased during the voltage pulse. Only transitions which lased in the afterglow were studied further as possible candidates for nuclear pumping. Laser output as a function of concentration was studied for afterglow lasing with the expectation that the optimum minority gas concentration in the electrical afterglow laser would also be optimum in the reactor created laser plasma.

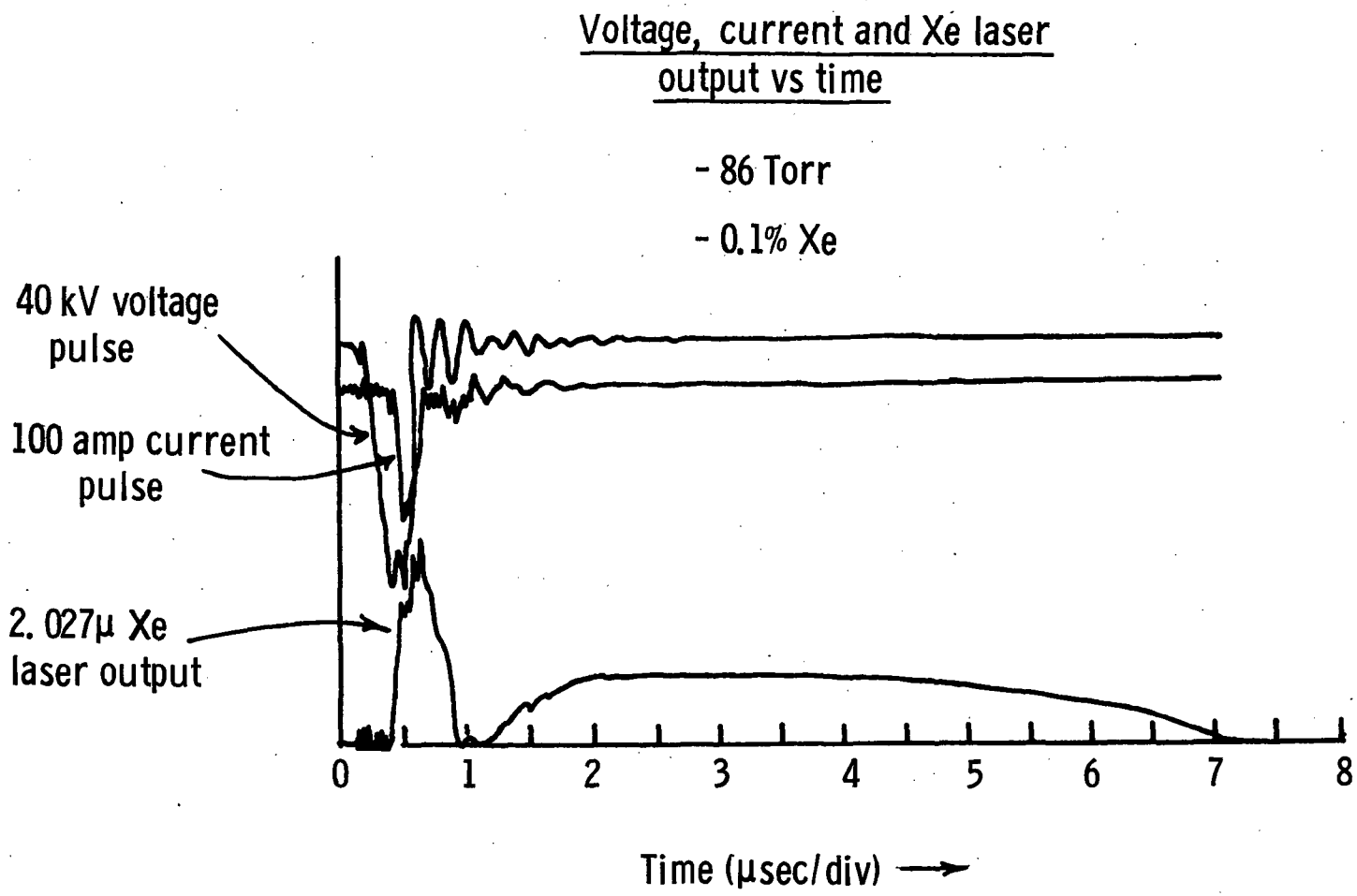
Voltage, current and Xe laser output vs time
- 86 Torr
- 0.1% Xe
40 kV voltage pulse
100 amp current pulse
2.027μ Xe laser output
0
1
2
3
4
5
6
7
8
Time (μsec/div) →

Fig. 3

The laser transitions studied are listed as follows:

He-Ar	1.79 μ	$3d[1/2]^0_1 - 4P[3/2]_2$
	1.27 μ	$3d^1[3/2]^0_1 - 4P^1[1/2]_1$
He-Xe	2.026 μ	$5d[3/2]^0_1 - 6P[3/2]_1$
He-Kr	2.52 μ	$4d[1/2]^0_1 - 5P[3/2]_2$
	2.19 μ	$4d[3/2]^0_2 - 5P[3/2]_2$
He-Ne	1.152 μ	$4S^1[1/2]^0_1 - 3P^1[3/2]_2$
	1.1177 μ	$4S[3/2]^0_2 - 3P[5/2]_3$
He-$F_2(NF_3)$	0.7129 μ	$3P\ ^2P^0_{1/2} - 3S\ ^2P_{1/2}$
	0.7311 μ	$3P\ ^2S^0_{1/2} - 3S\ ^2P_{3/2}$

All these transitions lase strongly in the afterglow except the FI laser where only weak afterglow lasing was observed. Figure 4 is an energy level diagram of major lasing transitions. Note that all of the minority species can be Penning ionized by the helium metastables.

The He-F_2 laser is of particular interest since it lases in the visible (higher energy photon than infrared trasitions, thus higher quantum efficiency) and also $^{235}UF_6$ could be used as the F donor . Future nuclear pumped lasers could be pumped by the $^{235}U(n,f)FF$ reaction and lase on the visible FI transitions. Figure 5 shows the current pulse, spontaneous emission and laser output of FI at 0.7129 μ vs. time. Note that if the laser pulse is expanded, lasing in the afterglow is found although weakly. This laser tends to be self-quenching due to the strong reabsorption of the spontaneous emission from the lower laser level of the ground state. The reabsorption may explain the shape of the afterglow laser pulse as well as why only weak afterglow lasing is observed.

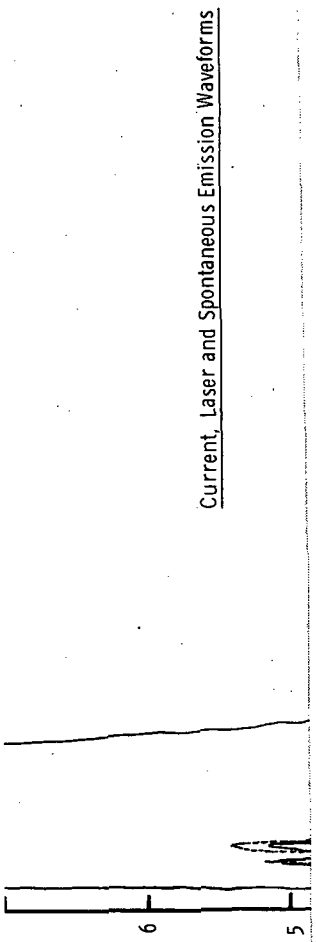
Current, Laser and Spontaneous Emission Waveforms
6
5

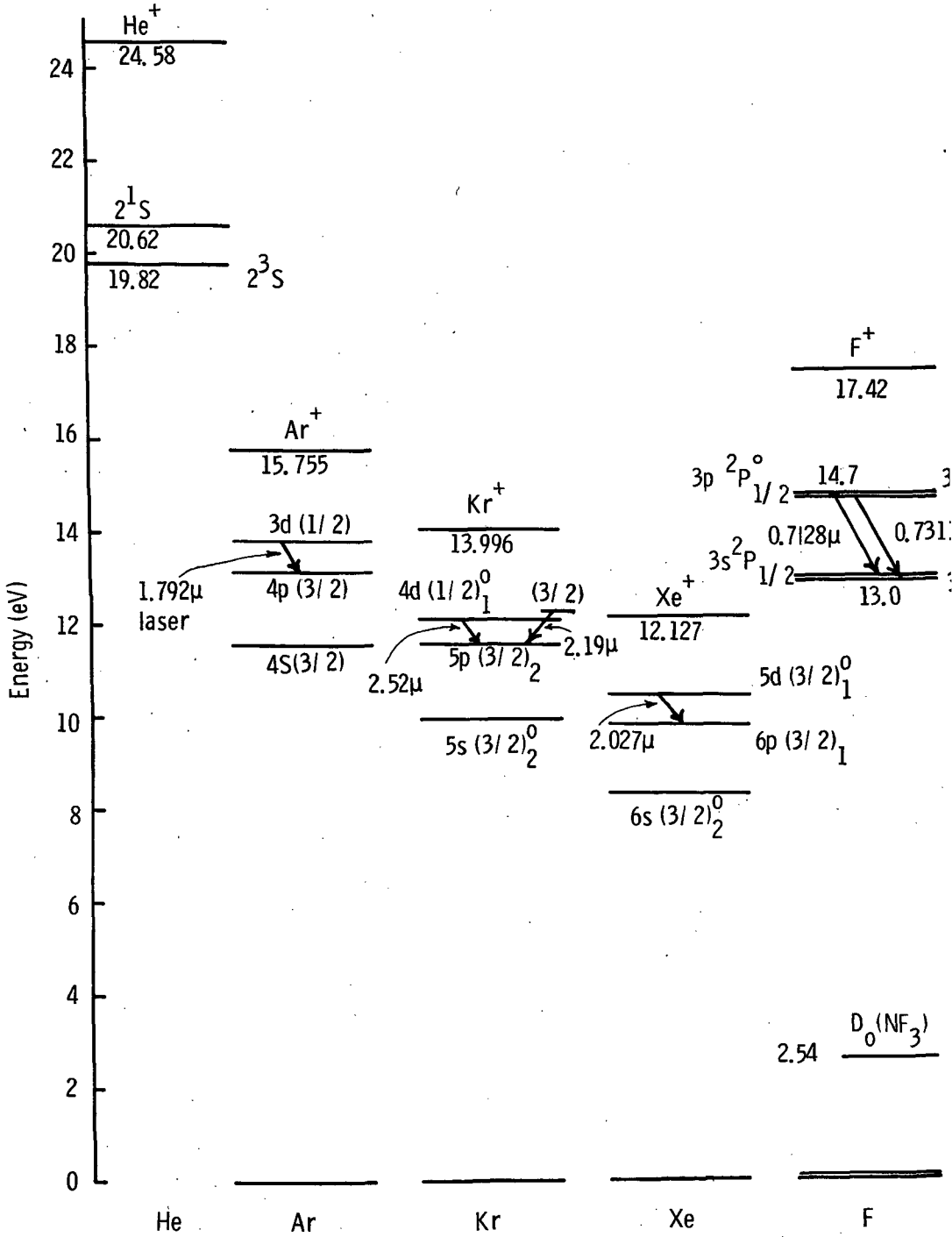
Energy (eV)
24
22
20
18
16
14
12
10
8
6
4
2
0
He+
24.58
2^1S
20.62
19.82
2^3S
Ar+
15.755
3d (1/2)
4p (3/2)
1.792μ
laser
4S(3/2)
Kr+
13.996
4d (1/2)^0_1
(3/2)
5p (3/2)_2
2.19μ
2.52μ
5s (3/2)^0_2
Xe+
12.127
5d (3/2)^0_1
2.027μ
6p (3/2)_1
6s (3/2)^0_2
F+
17.42
3p ^2P°_1/2
14.7
0.7128μ
0.731
3s^2P_1/2
13.0
D_0(NF_3)
2.54
He
Ar
Kr
Xe
F

Fig. 4

"Page missing from available version"

page 8.

NUCLEAR PUMPED REACTOR EXPERIMENTS

A. Nuclear Pumped Lasing Results

A high vacuum and gas handling system was constructed for use at the reactor site. This system was capable of 10^{-6} Torr and research grade gases were used in all experiments. The complete reactor system is shown in figure 6. The quartz laser cell is surrounded by a polyethylene moderator (15.24 cm dia. by 60 cm long) for thermalizing the fast neutrons from the Aberdeen fast-burst reactor. A small portion of the laser intensity was coupled out from the dielectric output laser mirror and then was absorbed by an InAr detector (1.2 μ - 3.5 μ transitions only). A filter wheel could be used to transmit only one wavelength of interest. The InAr detector was very insensitive to background gamma and fast-neutron irradiation.

Through the back laser cavity mirror, spectra was taken using an optical Multichannel analyzer. The data was plotted and placed on magnetic tape by a HP 9830 computer. Spectra of nearly all nuclear pumped laser discharges was taken in the range of 4000-8300Å.

Volumetric direct nuclear pumped lasing was first achieved in a ^{3}He-Ar mixture.[2,3] This was the first nuclear pumped laser to use the $^{3}He(n,p)^{3}H$ reaction as the excitation source. A typical oscilloscope trace of laser output during the thermal neutron pulse is shown in figure 7. Note the sharp laser threshold characteristics of all lasers. Lasing continues throughout the thermal neutron pulse. This profile is typical of both ^{3}He-Ar and ^{3}He-Xe nuclear pumped lasers. Nuclear pumping was achieved on both the 1.79 μ and 1.27 μ ArI transitions. The filter wheel was used for wavelength selection. The laser cavity consisted of a back mirror (flat), 99.5 percent reflective at 1.7 μ, and an output mirror (2-meter radius of curvature) with 1 percent transmission at 1.7 μ.

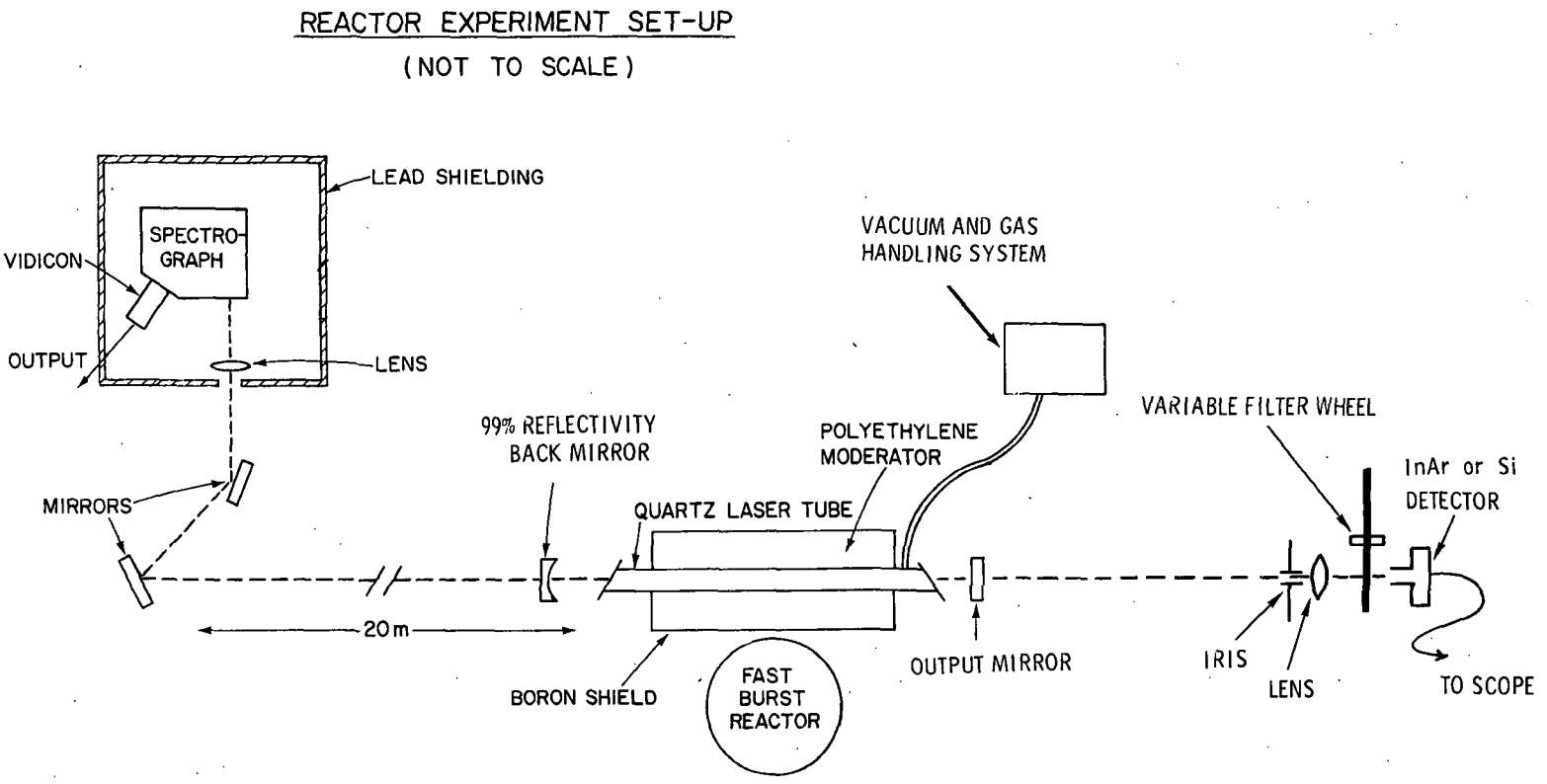
REACTOR EXPERIMENT SET-UP
(NOT TO SCALE)
LEAD SHIELDING
SPECTRO-GRAPH
VIDICON
OUTPUT
LENS
VACUUM AND GAS HANDLING SYSTEM
99% REFLECTIVITY BACK MIRROR
POLYETHYLENE MODERATOR
VARIABLE FILTER WHEEL
InAr or Si DETECTOR
MIRRORS
QUARTZ LASER TUBE
20 m
BORON SHIELD
FAST BURST REACTOR
OUTPUT MIRROR
IRIS
LENS
TO SCOPE

Fig. 6

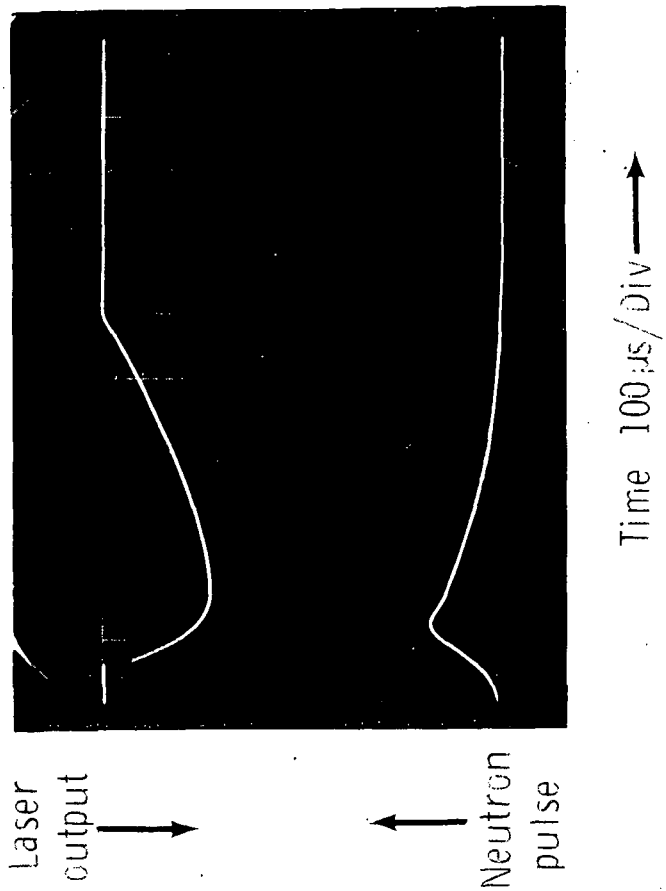

Fig. 7

Nuclear pumped lasing has also been achieved in ^{3}He-Xe at 2.026 μ.[4] This system has the advantage of having the lowest thermal neutron threshold flux of any volumetric nuclear pumped laser to date (4×10^{15} n/cm^2-sec). The laser cavity consisted of two 2-meter radius of curvature dielectric coated mirrors each having 97.5 percent reflectivity at 2 μ.

Figure 8 shows the scaling of 2.026 μ XeI laser output, the total pressure is held constant at either 600 or 400 Torr, as a function of thermal neutron flux. The solid lines are drawn through the two lower flux data points. If the laser output is directly proportional to the thermal neutron flux, then the upper data points should fall near the solid line, as they indeed do. No laser saturation effects were noted up to the maximum capable thermal flux of 1.5×10^{17} n/cm^2-sec.

The output laser mirror was changed from a 1 percent transmission mirror to a 20 percent transmission mirror in order to couple out more laser power. The results are shown in figure 9. The dashed curve shows laser output at 2.026 μ for the 1 percent transmission mirror. When the mirror was changed to 20 percent transmission, the solid curve resulted. With the 20 percent transmission mirror, the neutron flux threshold was higher but most importantly, there was not a substantial rise in power output. Thus, it appears that the 1 percent transmission undercoupled the cavity and the 20 percent transmission mirror overcoupled the laser cavity. Nevertheless, it can be concluded that the round-trip gain was greater than 20 percent.

In figure 10, the variation of ^{3}He-Ar and ^{3}He-Xe laser output is shown as a function of Ar or Xe concentration. Nuclear pumped lasing is shown by the circle or square data points and the solid or dashed lines represent the normalized Ar or Xe laser output from an electrically-pulsed afterglow laser (approximately 80 Torr total pressure). There is a very close correlation between electrically-pulsed afterglow lasing and nuclear pumped lasing. Thus, the major laser pumping processes must be the same in each case. These processes will be discussed in detail later.

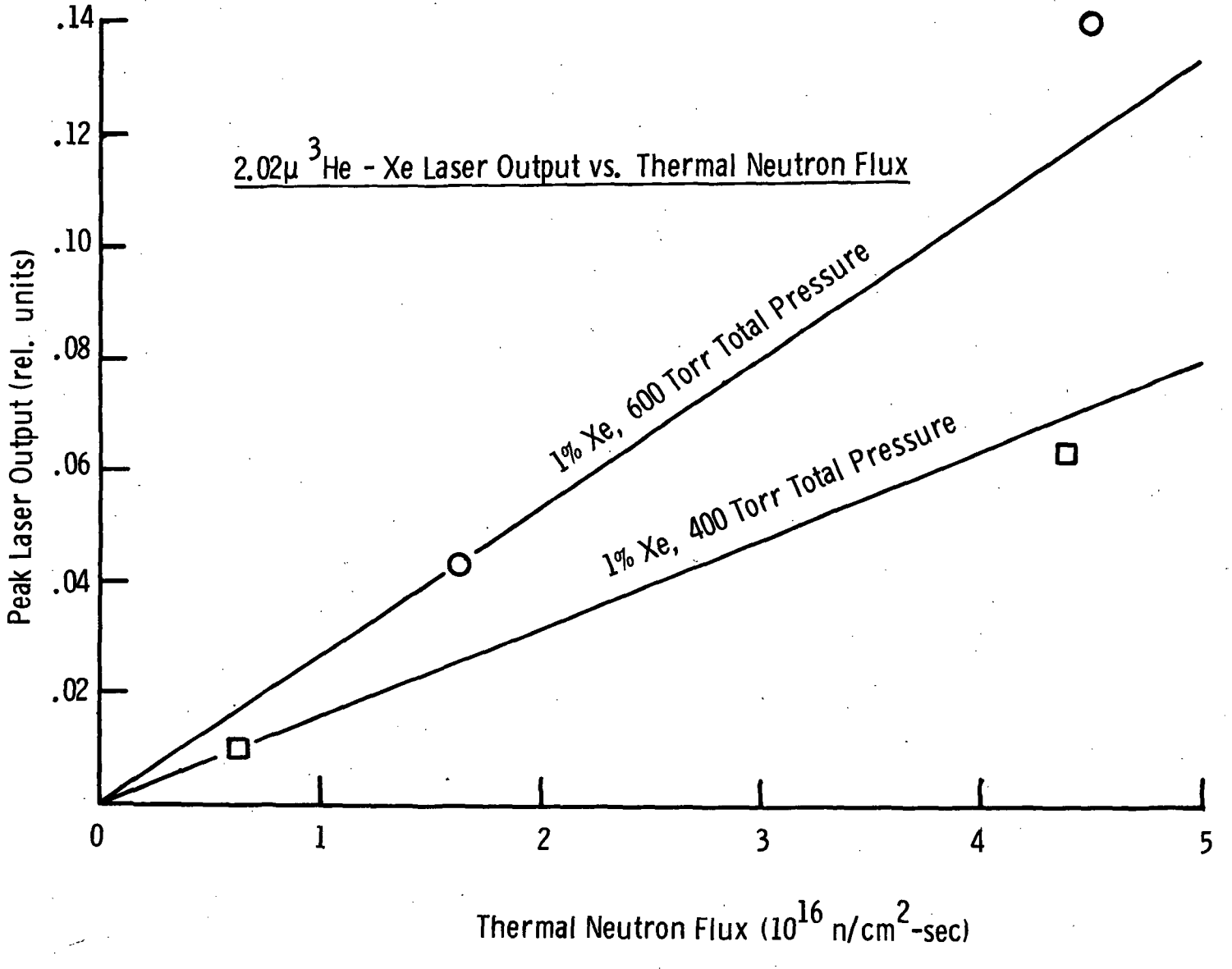
2.02μ ^{3}He - Xe Laser Output vs. Thermal Neutron Flux
Peak Laser Output (rel. units)
.14
.12
.10
.08
.06
.04
.02
0
1
2
3
4
5
Thermal Neutron Flux (10^{16} n/cm^2-sec)
1% Xe, 600 Torr Total Pressure
1% Xe, 400 Torr Total Pressure

Fig. 8

^{3}He-Xe Laser Output at 2.027μ
for 1% and 20% T Output Mirrors

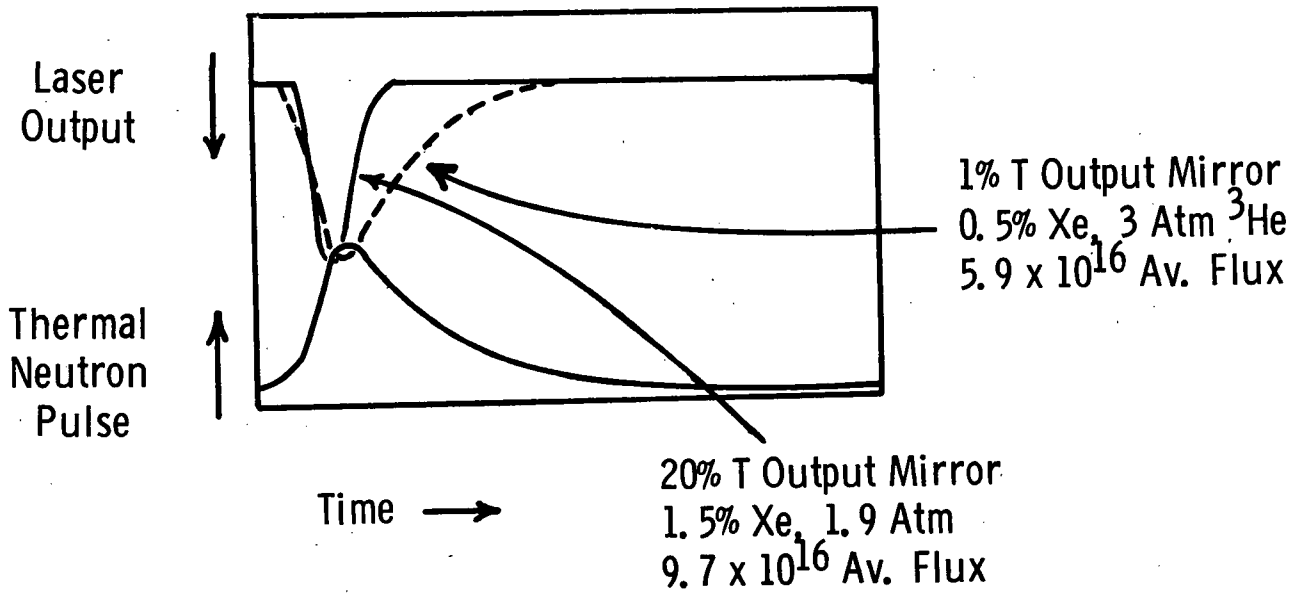

Fig. 9

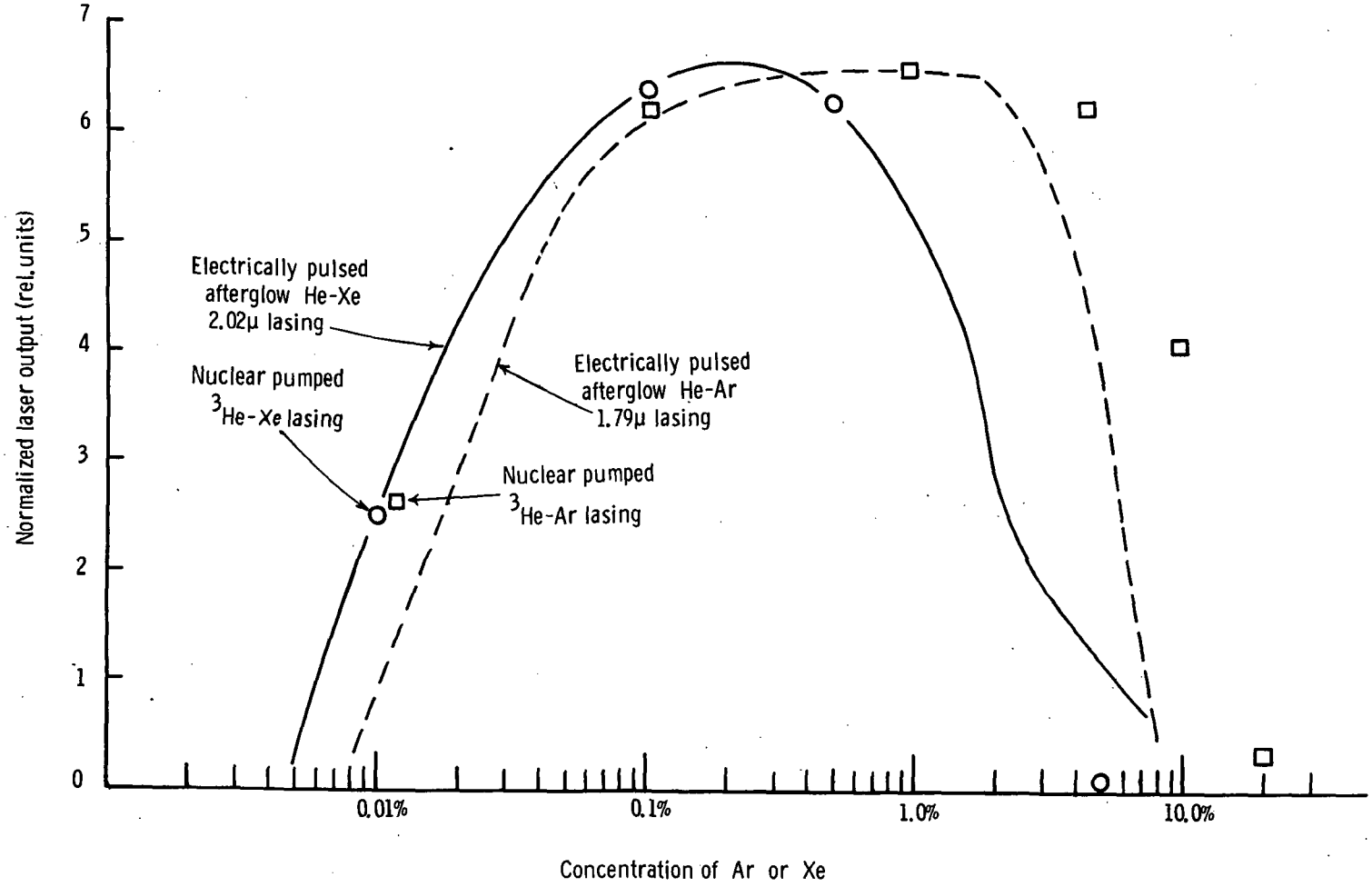
Normalized laser output (rel. units)
7
6
5
4
3
2
1
0
Electrically pulsed afterglow He-Xe 2.02μ lasing
Nuclear pumped ^{3}He-Xe lasing
Electrically pulsed afterglow He-Ar 1.79μ lasing
Nuclear pumped ^{3}He-Ar lasing
0.01%
0.1%
1.0%
10.0%
Concentration of Ar or Xe

Fig. 10

The peak nuclear pumped laser output is plotted in figure 11 as a function of total pressure in atmospheres. At the present time, the ^{3}He-Ar system has produced the greatest power output (3.7 watts). A thermal flux of 1×10^{17} n/cm^2-sec and an output mirror transmission of 1 percent was used. The ^{3}He-Xe system had approximately the same power output for both the 1 percent and 20 percent transmission output mirrors. Peak output was 370 mwatts at 4 atmospheres, 1×10^{17} n/cm^2-sec thermal flux.

In order to increase the power output of the ^{3}He-Xe system, 20 percent Ar was added. From electron beam experiments it has been shown that the addition of argon to a He-Xe mixture considerably enhances XeI laser output by the formation of Ar_2^* which is in close resonance to the XeI (2.026 μ) upper laser level. Thus, Ar_2^* can efficiently pump the 2.026 μ laser transition and as shown in figure 11, indeed increased the power output but only at pressures less than one atmosphere. As the total pressure increased, laser output decreased, eventually becoming zero at 4 atmospheres. Some other unknown detrimental effect quenches lasing at higher pressures.

In figure 12, the ^{3}He-Ar (1.79 μ) laser output is plotted as a function of total pressure (circle data points). The solid curve is the calculated power deposition (KW/cm^3) in the gas from the ^{3}He(n,p)^{3}H reaction. Both curves have been normalized at 2 atmospheres. Note that laser output follows the power deposited up to 2 atmospheres total pressure, but then tends to saturate as the pressure increases probably due to pressure broadening of the laser transition thus, lowering the gain. Optimum operation (optimum efficiency) occurs below 2 atmospheres for 1 percent Ar.

The efficiency is defined as the peak laser power output divided by the total power deposited in the laser cell. This gives an efficiency of 1.2×10^{-3} percent. If, instead of the total laser cell volume, the active mode volume (2 cm^2) is used, the efficiency becomes 0.09 percent.

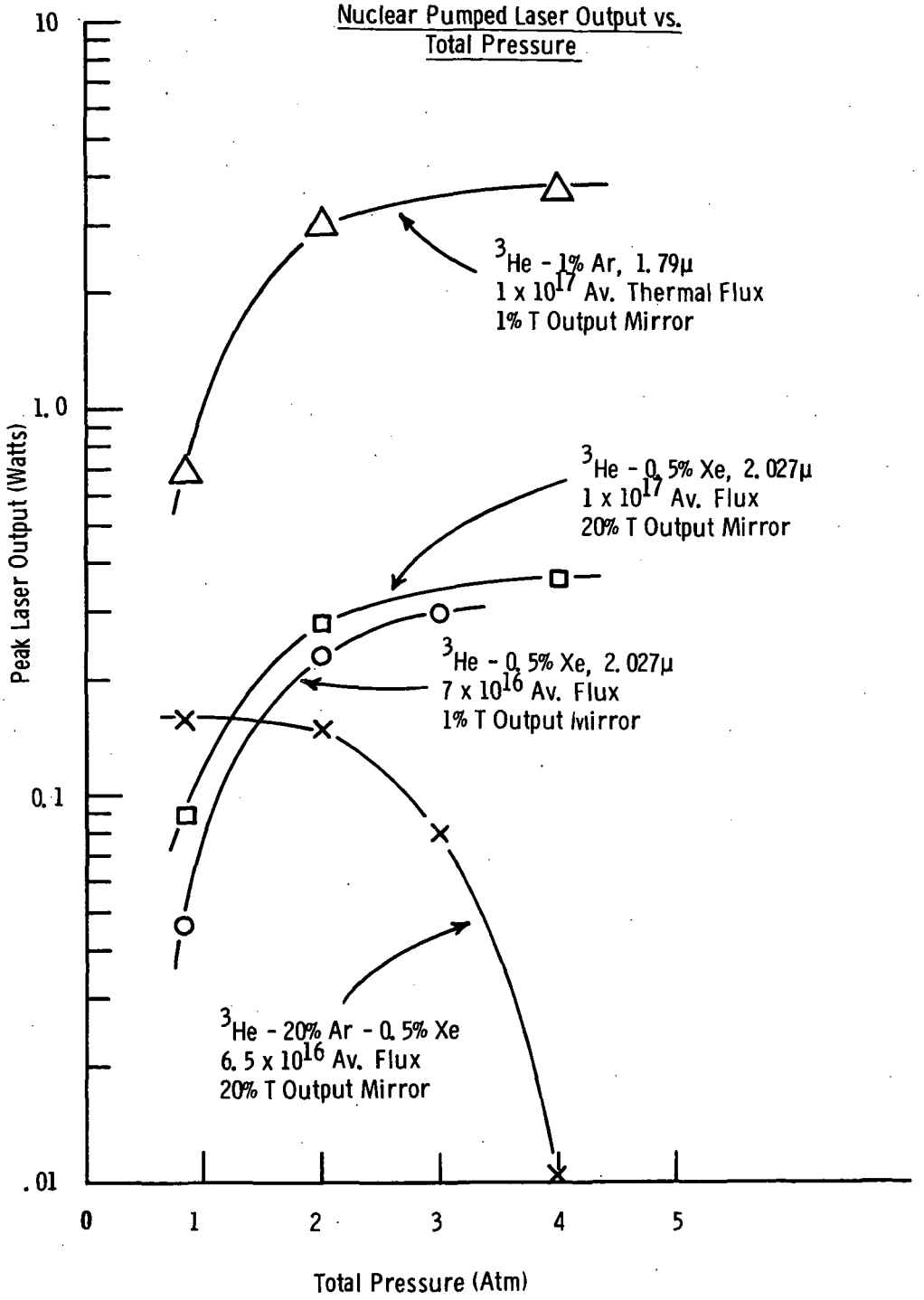
Nuclear Pumped Laser Output vs.
Total Pressure
10
1.0
0.1
.01
Peak Laser Output (Watts)
0
1
2
3
4
5
Total Pressure (Atm)
^{3}He - 1% Ar, 1.79μ
1 x 10^{17} Av. Thermal Flux
1% T Output Mirror
^{3}He - 0.5% Xe, 2.027μ
1 x 10^{17} Av. Flux
20% T Output Mirror
^{3}He - 0.5% Xe, 2.027μ
7 x 10^{16} Av. Flux
1% T Output Mirror
^{3}He - 20% Ar - 0.5% Xe
6.5 x 10^{16} Av. Flux
20% T Output Mirror

Fig. II

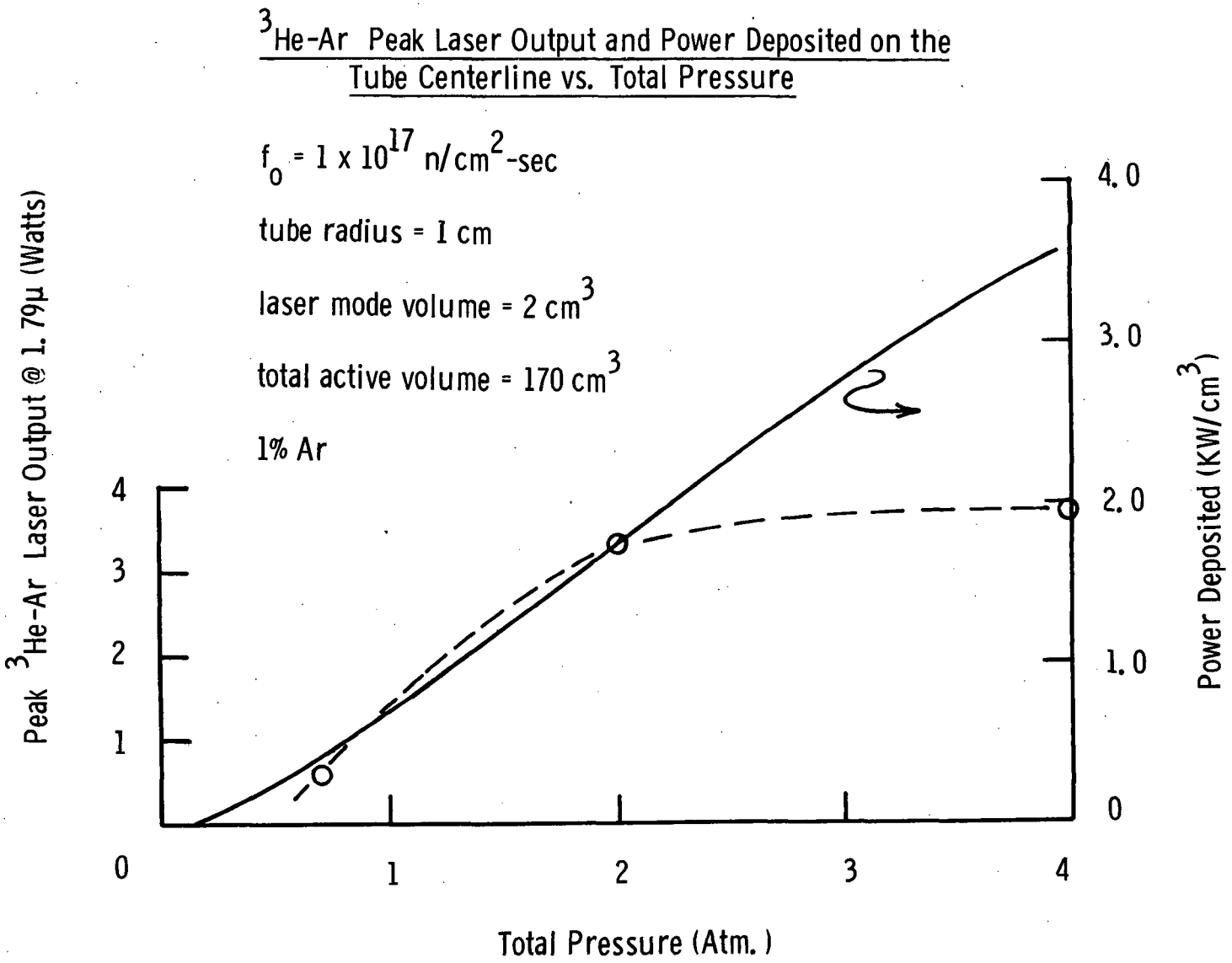
^{3}He-Ar Peak Laser Output and Power Deposited on the Tube Centerline vs. Total Pressure
$f_o = 1 \times 10^{17}$ n/cm^2-sec
tube radius = 1 cm
laser mode volume = 2 cm^3
total active volume = 170 cm^3
1% Ar
Peak ^{3}He-Ar Laser Output @ 1.79μ (Watts)
Power Deposited (KW/cm^3)
Total Pressure (Atm.)
0
1
2
3
4
0
1.0
2.0
3.0
4.0

Fig. 12

The ^{3}He-Kr nuclear pumped laser output is shown in figure 13. This system has a very high thermal neutron flux laser threshold as noted from the figure. This is probably due to the fact that both the 2.52 μ and 2.19 μ laser transitions have the same lower laser level (see figure 4). Both these transitions lase in the reactor plasma, thus populating the lower laser level which quenches further lasing (or produces a high laser threshold). No further investigations were undertaken on this system due to this observation.

Nuclear pumped lasing was also achieved in a mixture of ^{3}He-Ne (1 percent Ne) at 400 Torr total pressure with a peak thermal flux of 7.6×10^{15} n/cm^2-sec. As yet, we have not determined the lasing wavelength but most probably it is either the 1.15 μ or the 1.1177 μ NeI transitions. Further investigation of this system will pinpoint the lasing wavelength.

Nuclear pumped lasing of FI has been investigated. This system is of particular interest since it is very compatible with UF_6. The electrically-pulsed FI laser operates equally well with F_2, NF_3 or UF_6, each simply acts as a fluorine donor. The fluorine in turn is excited to the upper laser level by direct electron impact excitation, and, or by excitation transfer from the high density helium metastables.

A ^{3}He-NF_3 mixture (0.14 percent NF_3) was used at a total pressure of 570 Torr for studies at the reactor. The peak thermal neutron flux was approximately 7×10^{16} n/cm^2-sec. As shown in figure 14, two distinct spontaneous emission peaks are noted at 7129Å and 7311Å on the optical multichannel analyzer. These two wavelengths correspond to FI lasing wavelengths found in laboratory investigations of He-NF_3 mixtures under electrical excitation. Nuclear pumping was also investigated for a 1 percent NF_3 gas fill, but as noted in figure 14, no spontaneous emission was found.

Nuclear pumped lasing in FI has <u>not</u> been achieved as yet. A range of thermal fluxes as high as 1.2×10^{17} n/cm^2-sec have been used at total pressures of 600 Torr ^{3}He-NF_3. One interesting effect was noted, when the percentage of NF_3 was very low ($\sim$ 0.008 percent), substantially more total light was emitted from the tube than at 1 percent NF_3 (also note same effect on fig. 14). Thus, it appears that fluorine effectively quenches the plasma, probably by absorbing low energy electrons to form F^-. This in turn reduces the number of low energy electrons available for recombination with He^+, He_2^+, Ar^+, etc. But if the NF_3 concentration is kept low, the formation rate of F^- is low and recombination light results.

The FI laser is a classic three-level system. Thus, strong reabsorption of the spontaneous emission takes place between the ground state of F and the lower laser level, effectively quenching lasing in the electrical afterglow. This is probably the reason that the FI system and similar such systems are not good candidates for nuclear pumping.

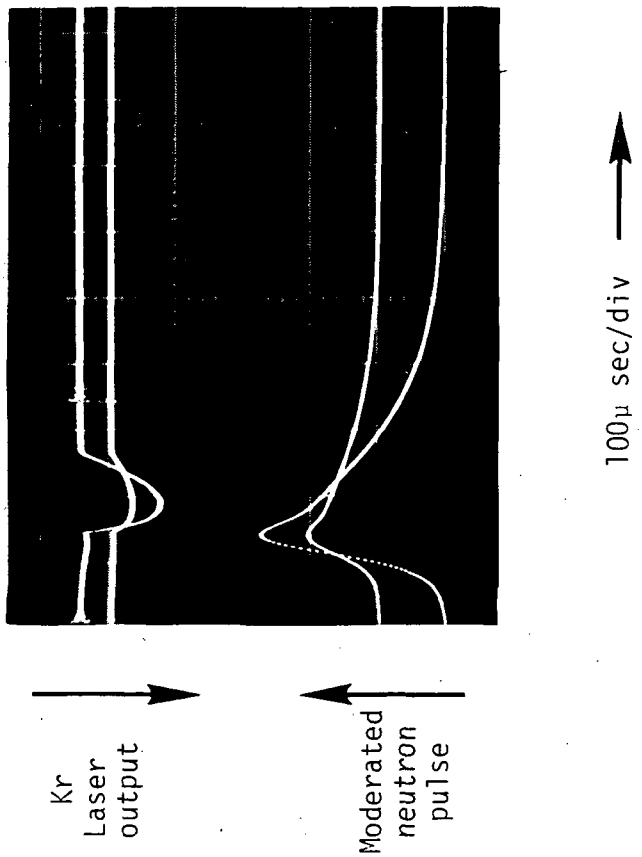

Fig. 13

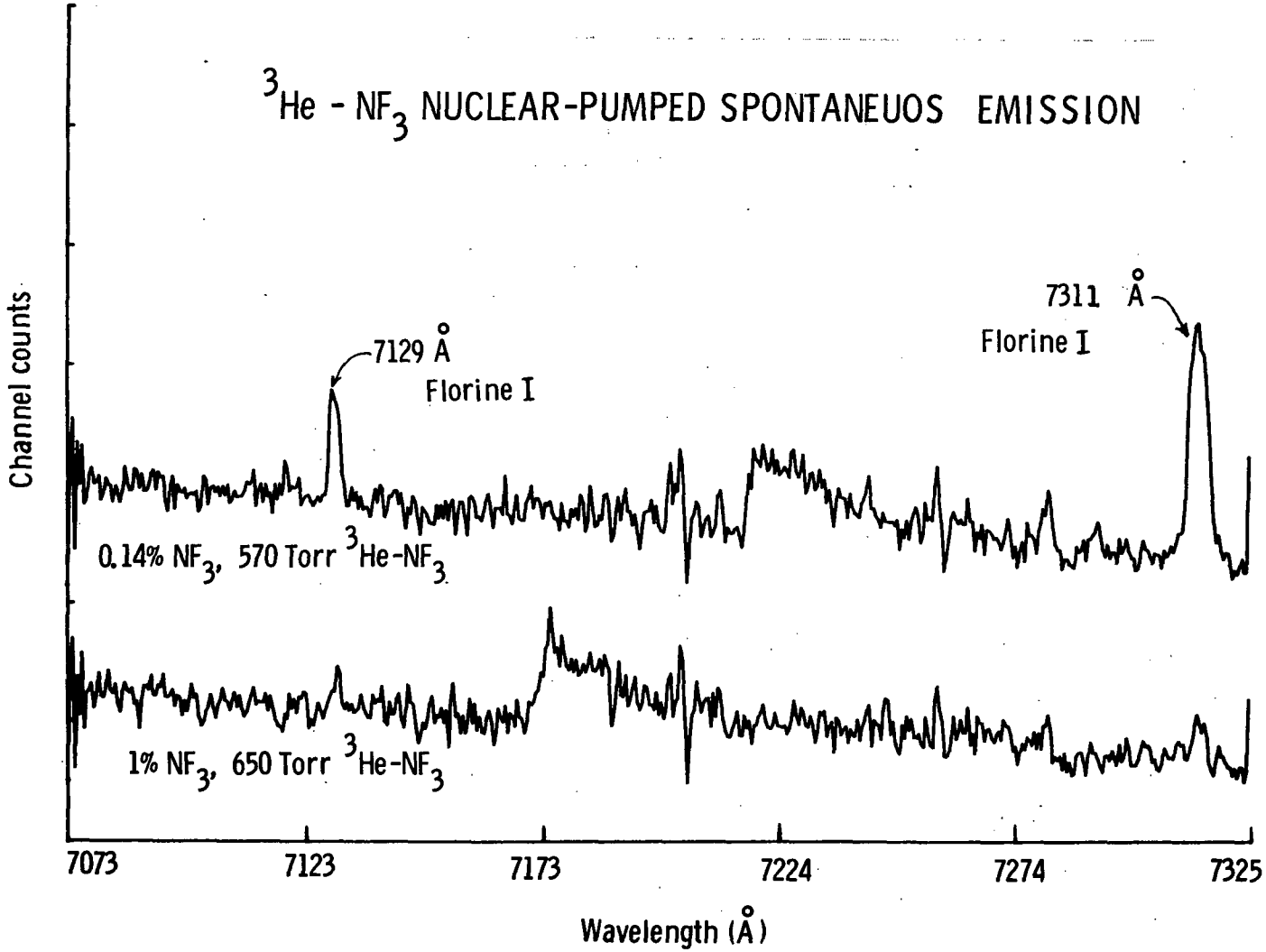
^{3}He - NF_3 NUCLEAR-PUMPED SPONTANEUOS EMISSION
Channel counts
7129 Å
Florine I
7311 Å
Florine I
0.14% NF_3, 570 Torr ^{3}He-NF_3
1% NF_3, 650 Torr ^{3}He-NF_3
7073
7123
7173
7224
7274
7325
Wavelength (Å)

Fig. 14

Another system under active investigation is the He-Xe-NF_3 system or excimer laser XeF^* (3550Å). Lasing has not been achieved under electrical excitation as yet, but the XeF^* excimer emission has definitely been observed. Figure 15 shows the XeF^* emission under nuclear excitation with 1 percent Xe, 1 percent NF_3 and a total pressure (^{3}He-Xe-NF_3) of 2 atmospheres. The XeF^* excimer emission at 3511 and 3531Å is observed. When a high-Q optical cavity was placed around the nuclear discharge no lasing was noted at a thermal flux of 6.7×10^{16} n/cm^2-sec. This system will be further investigated at the reactor.

B. Nuclear Laser Pumping Processes

To optimize a laser system for maximum power output as well as evaluating new laser systems, it is important to understand the basic processes occurring in the charged particle produced laser plasma. The first system to be extensively investigated was the ^{3}He-Ar system. Figure 16 shows the major process thought to occur in the nuclear-generated plasma. Since the majority of the gas is helium ($\sim$ 99 percent), most of the excitation goes into the helium as compared to the argon minority gas.

Helium is first ionized by the secondary electrons produced by the $^3He(n,p)^3H$ reaction charged particles. The He atomic ions can form He_2^+ which eventually decay into atomic He metastables, or the atomic ion can by collisional radiative recombination recombine to form metastables. Large densities of these metastables can be obtained as shown by the work of Guyot.[1] The He metastablesthen collide with ground state argon and ionize it (Penning ionization). Argon ions can also be formed by direct electron impact ionization by secondary electrons, but this is thought to be of secondary importance as compared to Penning ionization. Once the atomic ion is formed, it can either recombine by collisional radiation recombination and then radiatively decay into the upper laser level or it can form, by association with two ground state Ar's, Ar_2^+ molecules. Ar_2^+ has a large dissociative recombination coefficient, thus upon recombination forms a ground

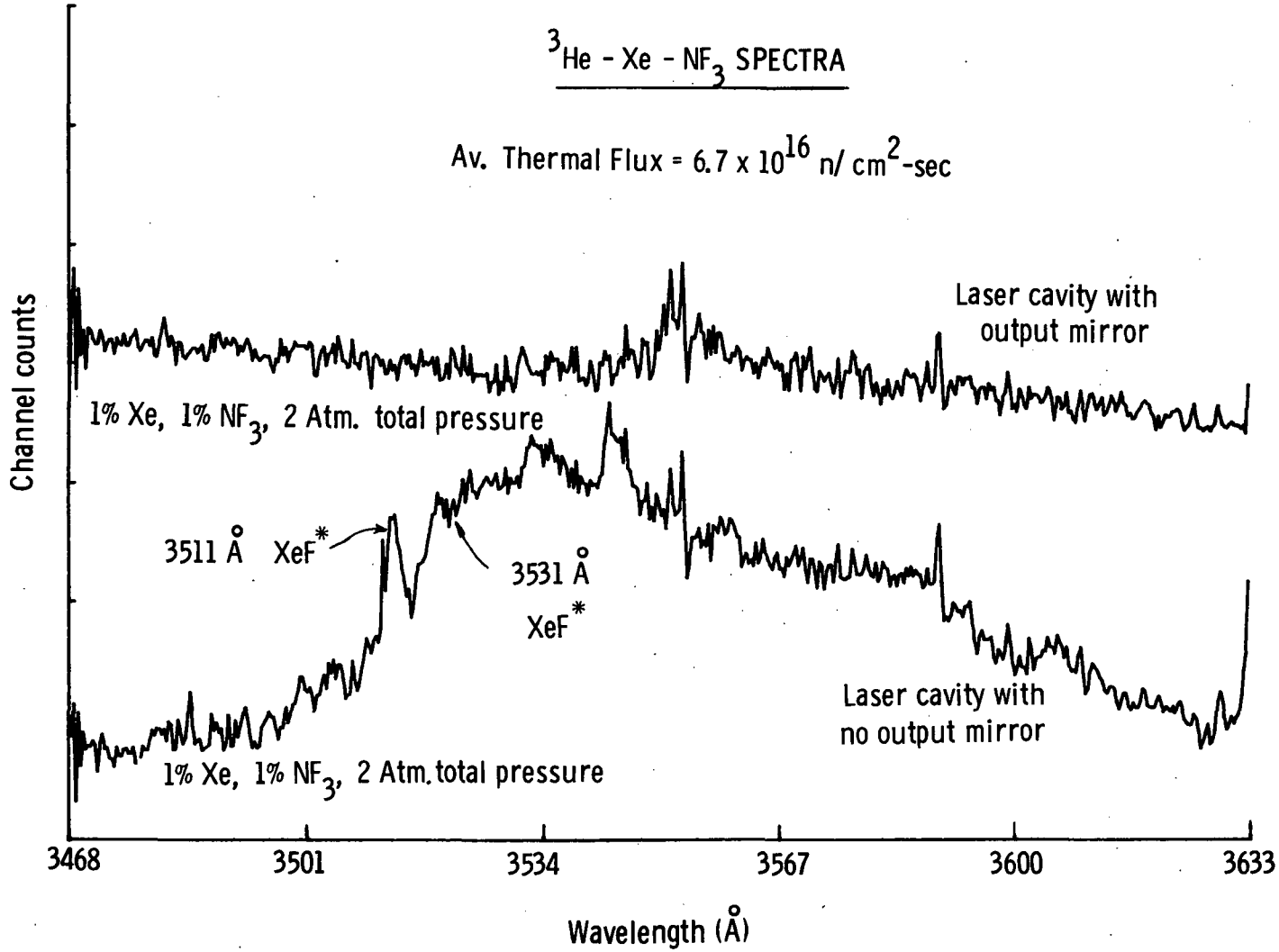
^{3}He - Xe - NF_3 SPECTRA
Av. Thermal Flux = 6.7 x 10^{16} n/ cm^2-sec
Channel counts
Laser cavity with output mirror
1% Xe, 1% NF_3, 2 Atm. total pressure
3511 Å XeF*
3531 Å XeF*
Laser cavity with no output mirror
1% Xe, 1% NF_3, 2 Atm. total pressure
3468
3501
3534
3567
3600
3633
Wavelength (Å)

Fig. 15

Collisional Processes in ^{3}He-Ar DNP Laser

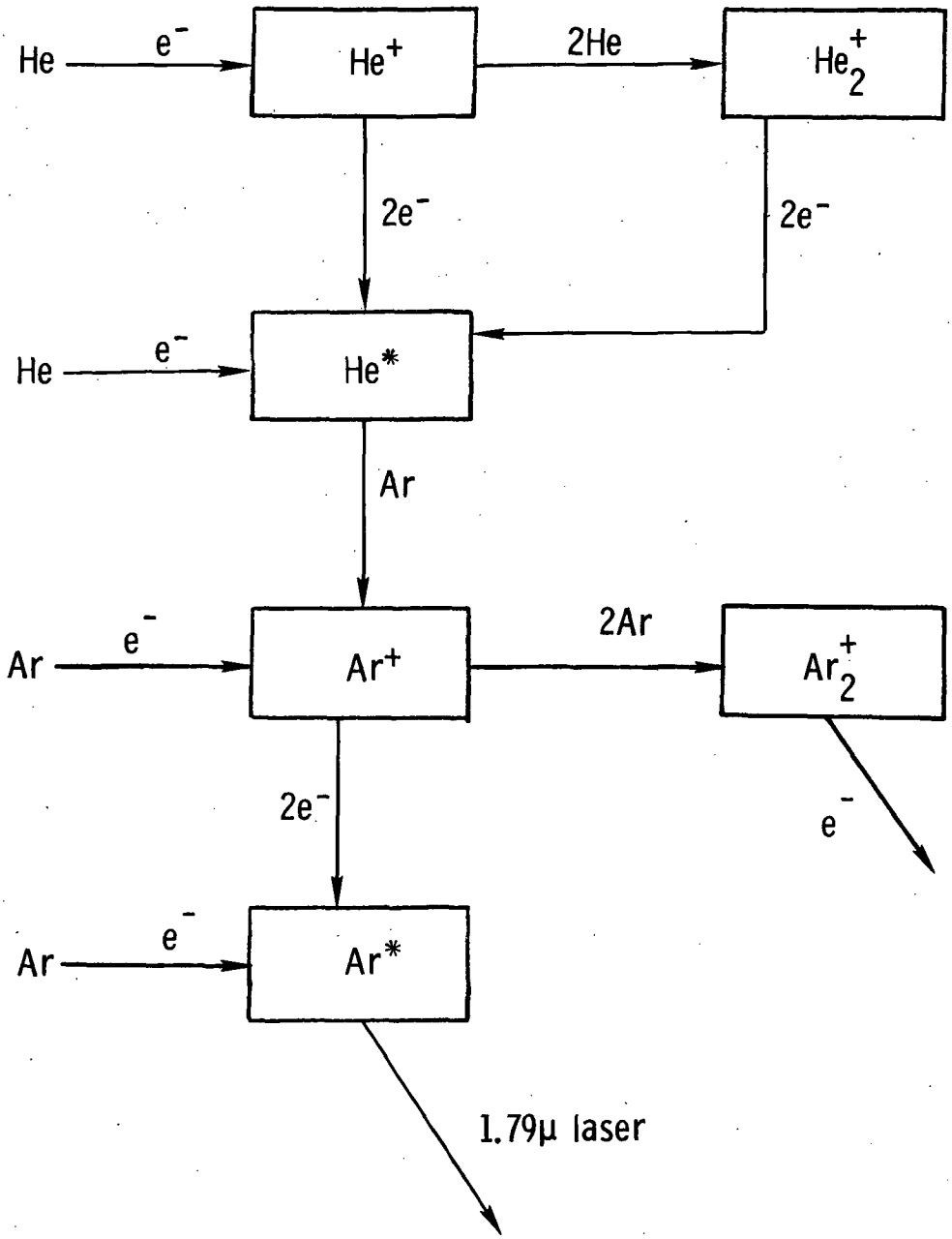

Fig. 16

state Ar and an excited Ar^*. The important point is that this excited Ar^* species is below the upper laser level for 300°K plasmas and thus does not contribute to the 1.79 μ ArI lasing. Formation of Ar_2^+ is simply considered as a loss term for Ar^+ and in turn the upper laser level density. The concentration of Ar must be kept low in order to retard the formation of Ar_2^+ but not so low that an insufficient upper laser level population results.

A simple computer program was written to solve the following equation for the Ar^+ density. It is assumed that the upper laser level density will follow the Ar^+ density.

$$\frac{dAr^+}{dt} = [He(m)][Ar]K_1 + [e^-][Ar]K_2 - [Ar^+][Ar][He]K_3$$
$$- [e^-]^2[Ar^+]K_4 - [Ar^+][Ar]^2K_5 = 0$$

A steady-state He(m) (metastable) density of $10^{12}cm^{-1}$ and an electron density of 10^{11} cm^{-1} is assumed based on the work of J. Guyot.[1] The total pressure was held constant at 400 Torr. The results of the calculation are shown in figure 17. The He-Ar (1.79 μ) nuclear laser output has been normalized to the Ar^+ density at 0.1 percent Ar concentration. There is a very close fitting of the experimental data points by the solution of the above equation which supports the explanation of the basic processes as given above. Note the strong decrease in laser output as the argon concentration increases due to the formation of Ar_2^+.

The basic processes just described can also be used to describe nuclear pumped lasing in He-Xe (2.026 μ). Of particular interest is a recent paper by Shiu, Biondi and Sipler[5] in which a 20 Torr Xe afterglow plasma (Te = Tg = 300°K) was created to study the specific atomic states excited after dissociation recombination of Xe_2^+. These atomic states are shown in figure 18. When the plasma was 300°K, the solid line transitions were observed. The thicker the line the more intense the transition (the more populated the state). Note that very strong

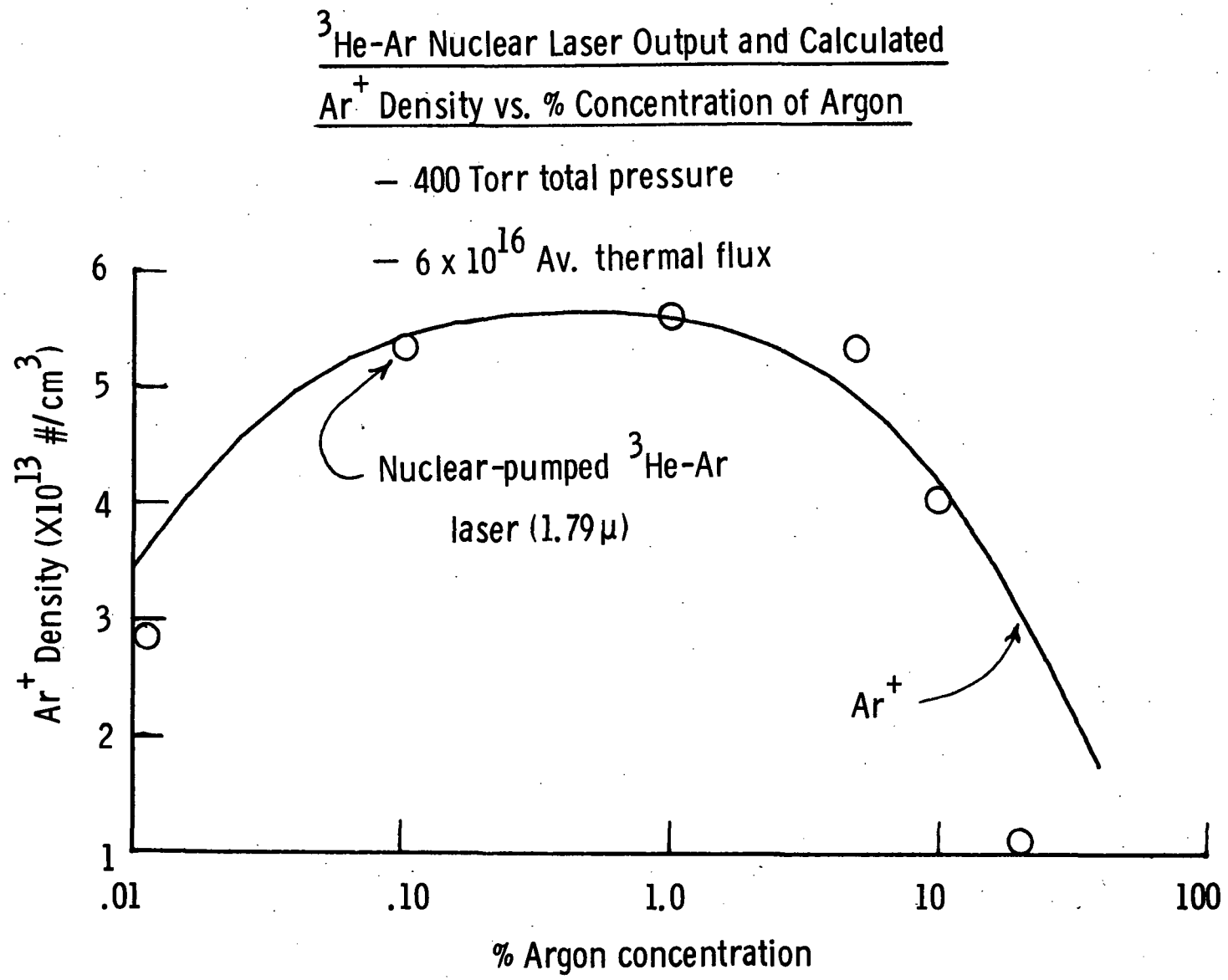
^{3}He-Ar Nuclear Laser Output and Calculated
Ar^+ Density vs. % Concentration of Argon
— 400 Torr total pressure
— 6×10^{16} Av. thermal flux
Ar^+ Density ($X10^{13}$ #/cm^3)
6
5
4
3
2
1
Nuclear-pumped ^{3}He-Ar
laser (1.79 μ)
Ar^+
.01
.10
1.0
10
100
% Argon concentration

Fig. 17

Dissociative Recombination in Xenon

- Shiu, Biondi, Sipler, Phys. Rev. A, Feb. 1977
- 20 Torr Xe
- Te = Tg = 300°K

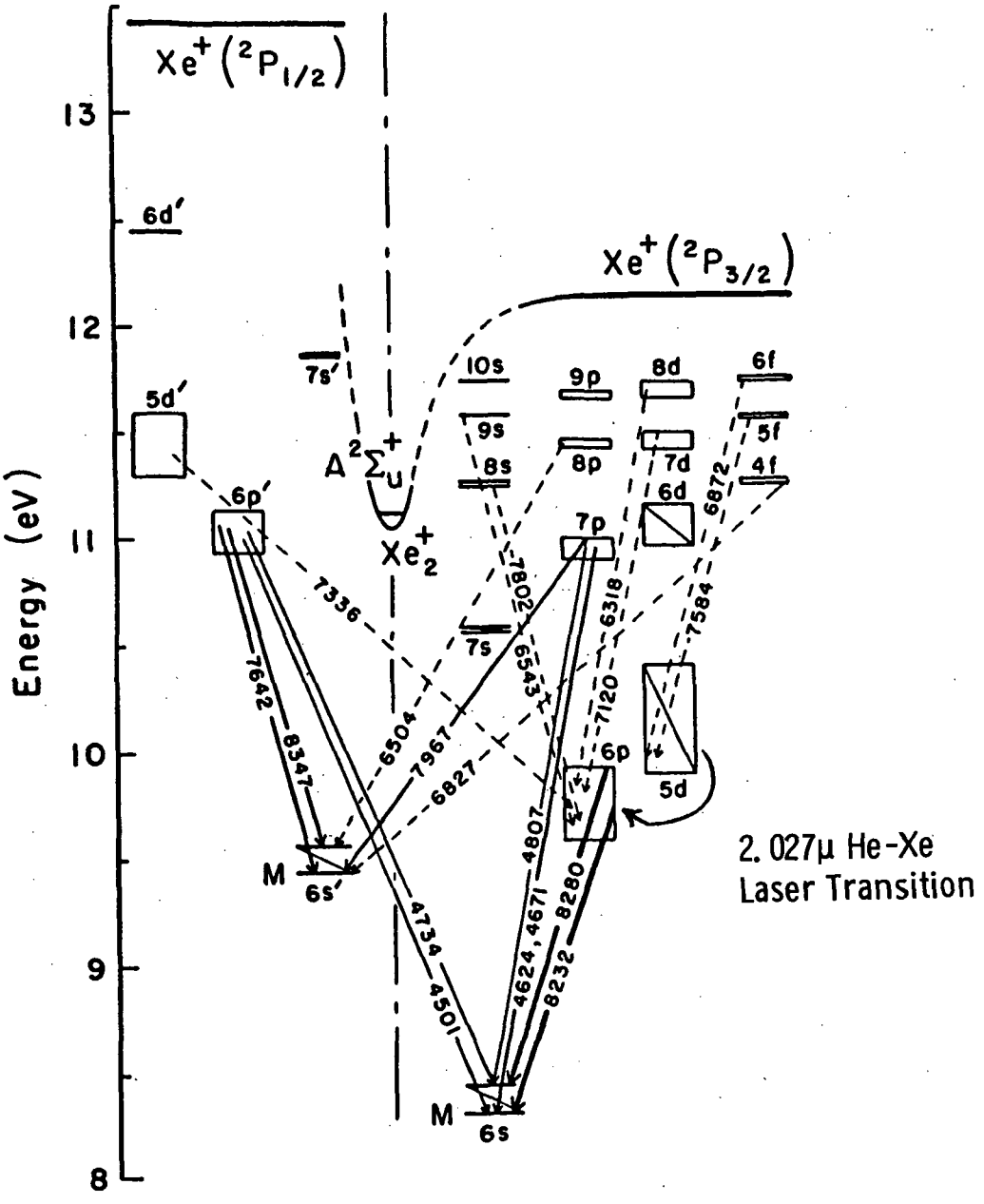

Fig. 18

transitions occur between the 6P and 6S atomic levels. The 6P levels correspond to the lower laser level of the XeI (2.026 μ) laser transition, thus dissociative recombination directly feeds the lower laser level which in turn helps quench lasing. Their experimental apparatus will not allow observation of transition out of the 5d upper laser level which is possibly also being fed by dissociative recombination. The significant point is that the lower laser level is definitely being populated by dissociative recombination of Xe_2^+.

BASIC STUDIES WITH UF_6

It would be very advantageous to directly couple the nuclear pumped laser with the reactor neutron source. This can be accomplished if the neutron source is a gas-core reactor. Under this concept, the reactor would be some mixture of helium or argon and $^{235}UF_6$ gases at high pressures. The $^{235}UF_6$ would provide a self-critical system and the energy would be coupled out as high-power, directional laser light. Thus, we have a self-critical direct nuclear pumped laser.

At the present time, it does not appear that the UF_6 molecule will lase on some vibrational or rotational level, nevertheless the UF_6 would be used as a fluorine donor. Thus, systems such as He-F (∿ 7000Å) or the XeF^* (∿ 3500Å) excimer became very attractive.

Using a specially designed vacuum system, mixtures of He and F_2 or UF_6 were electrically pulsed. Lasing was achieved on both the 7129Å and 7311Å FI lines in F_2 and UF_6 mixtures. Thus, it is possible to use UF_6 to achieve lasing, where the UF_6 simply supplies a free fluorine atom to be excited by either the helium metastables or by direct electron impact excitation.

The effect of UF_6 added to a He-Xe (2.026 μ) electrically-pulsed afterglow laser was studied. It was found that as much as 5 percent UF_6 could be added to a He-Xe (0.5 percent Xe) mixture before afterglow lasing would cease. This same experiment was attempted at the reactor by adding 1 percent, then 0.5 percent UF_6 to a ^{3}He-Xe (1 percent Xe) nuclear laser at a total pressure of 600 Torr. No XeI nuclear lasing was found even for UF_6 concentrations of 0.5 percent. Thus, it may prove very difficult to add even small quantities of UF_6 to other laser systems. This result is similar to that found earlier in the ^{3}He-NF_3 reactor experiments, where 1 percent NF_3 quenched the total light output. The UF_6 molecule or its dissociation products must be used directly to achieve lasing as well as a means of energy deposition.

CALCULATION OF CHARGED PARTICLE ENERGY DEPOSITION IN He GAS

In order to determine nuclear laser efficiency, the power deposited in the gas by the $^3He(n,p)^3H$ reaction had to be calculated. This has resulted in a paper by DeYoung and Winters to be published in the Journal of Applied Physics, August 1977.[6] Two other papers will soon be released by Wilson and DeYoung which cover power deposition in He by the $^{235}UF_6(n,f)FF$[7] reaction as well as the $^3He(n,p)^3H$[8] reaction.

In figure 19 is shown the results of the calculation done by DeYoung and Winters[6] of power deposition in ^{3}He for the nuclear pumped lasers described earlier. The energy deposited is made up from the slowing down of both the proton and tritium ions. The maximum operating pressure to date has been about 3000 Torr, but as noted from figure 19 at higher pressure, more power can be deposited. Above 6000 Torr, the power deposition falls due to the high thermal neutron attenuation; thermal neutrons can no longer reach the laser cell centerline, thus power deposition on the centerline falls. This effect can be overcome by using smaller diameter laser cells.

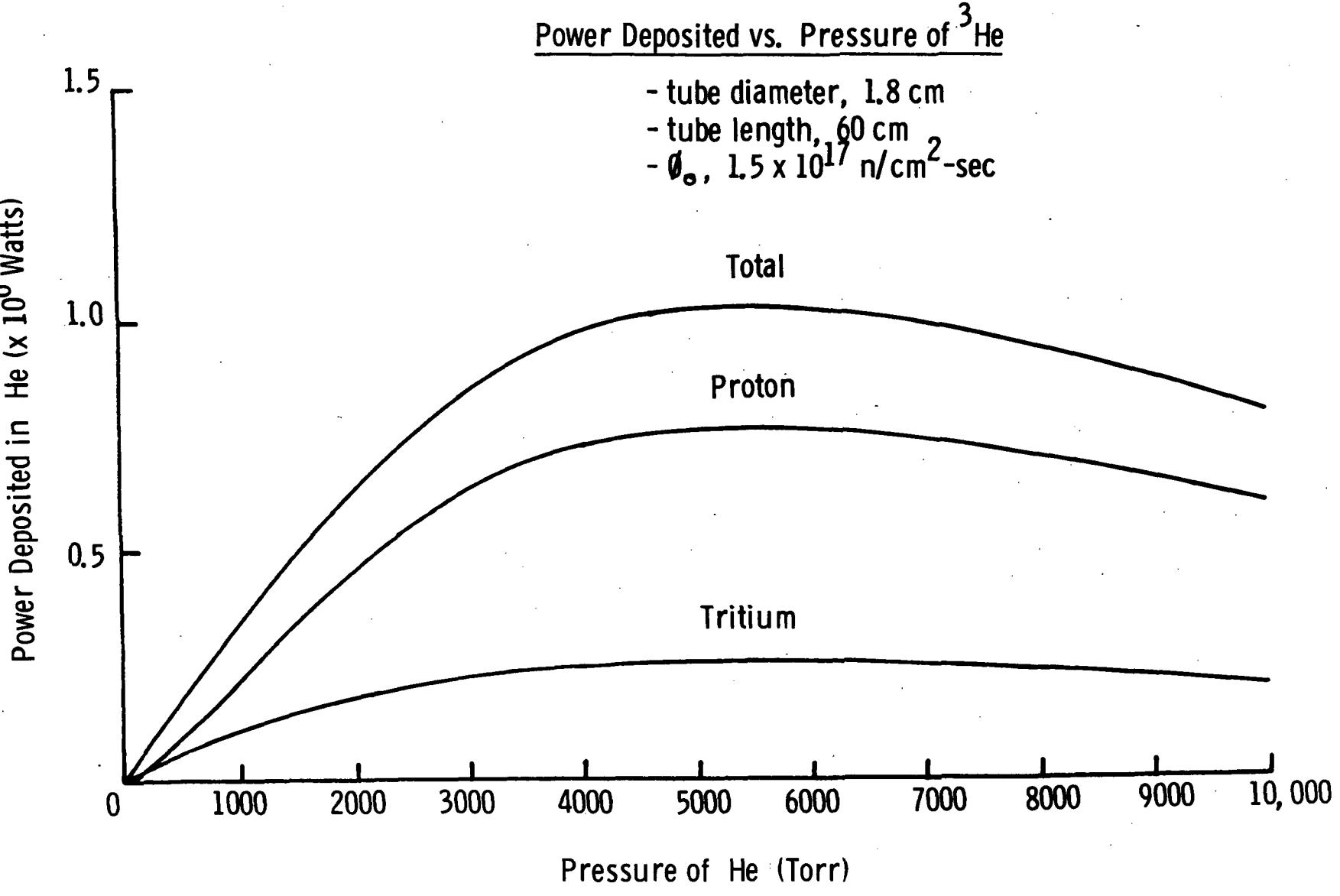
Power Deposited vs. Pressure of ^{3}He
- tube diameter, 1.8 cm
- tube length, 60 cm
- ϕ_o, 1.5 x 10^{17} n/cm^2-sec
Total
Proton
Tritium
Power Deposited in He (x 10^6 Watts)
1.5
1.0
0.5
0
1000
2000
3000
4000
5000
6000
7000
8000
9000
10,000
Pressure of He (Torr)

Fig. 19

The design conditions (tube radius and ^3He pressure) for optimum power deposition in ^3He are shown in figure 20. For each operating pressure, there is an optimum tube radius for maximum power deposition. The upper and lower 10 percent limits describe the region in which at least 90 percent of the available power is deposited in the gas volume.

CONCLUSIONS

The major accomplishments achieved under NASA Grant NSG-1232 can be summarized as follows:

1. Volumetric direct nuclear pumping has been achieved using the $^3He(n,p)^3H$ reaction in ^3He-Ar, ^3He-Xe, ^3He-Kr, and ^3He-Ne.

2. Scaling of laser output with thermal neutron flux has shown that output is directly proportional to flux.

3. Scaling with ^3He pressure up to approximately 4 atmospheres has shown that laser output follows the power deposited up to 2 atm then tends to saturate at higher pressures.

4. A maximum laser output power of 3.7 watts has been obtained from ^3He-Ar (1.79 μ) at 4 atmospheres total pressure (1 percent Ar).

5. Laboratory results have shown that the electrically-pulsed afterglow laser can be used to study and optimunize the nuclear or charged particle produced laser.

6. Nuclear pumped lasing (2.026 μ) and spontaneous emission are efficiently quenched with either small concentrations of UF_6 or NF_3. UF_6 can be used as an F donor for such systems as XeF* or KrF*.

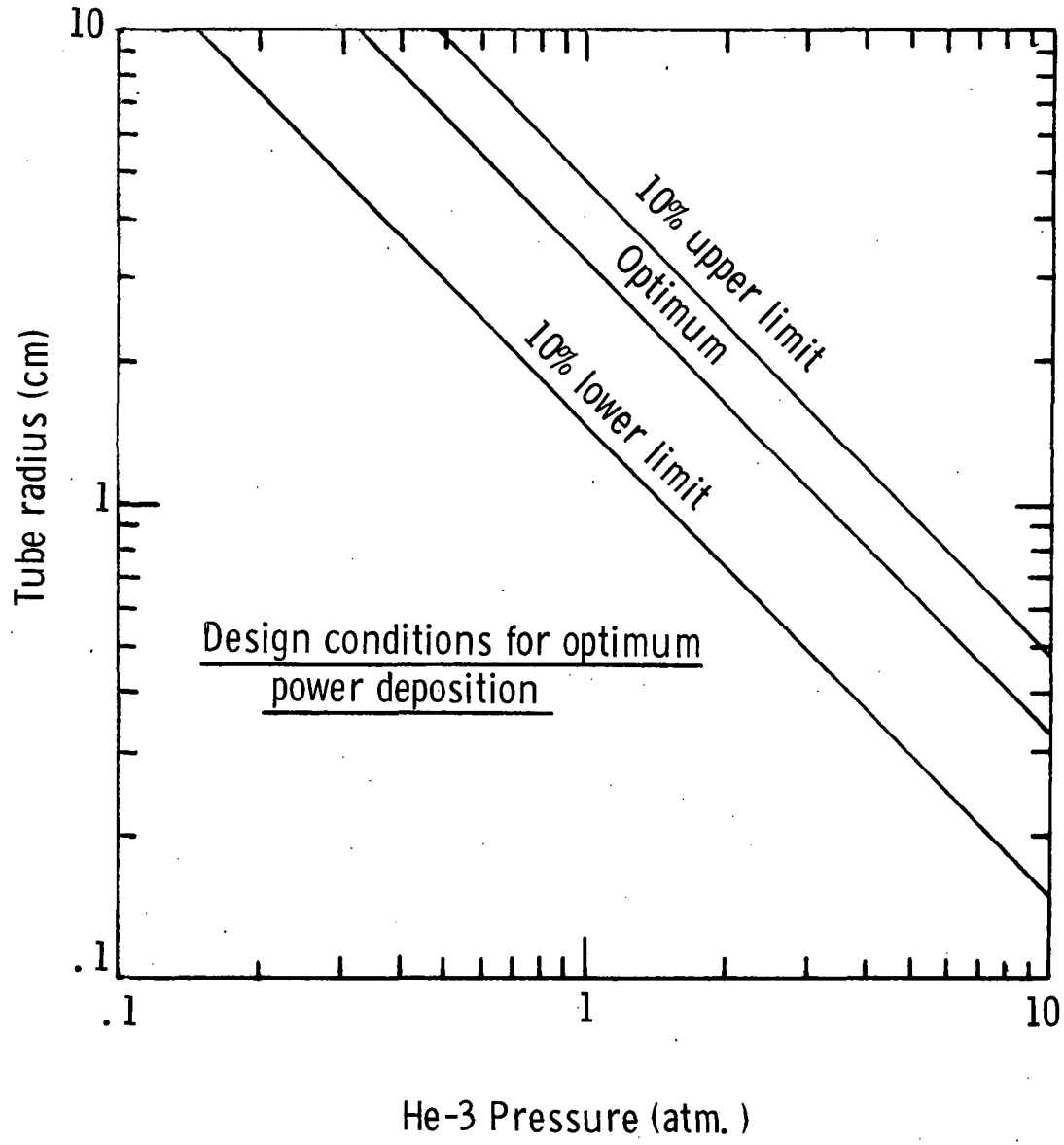
10
1
.1
.1
1
10
Tube radius (cm)
He-3 Pressure (atm.)
10% upper limit
Optimum
10% lower limit
Design conditions for optimum
power deposition

Fig. 20

REFERENCES

1. J. C. Guyot, Measurement of Atomic Metastable Densities in Noble Gas Plasmas Created by Nuclear Reactions, Univ. of Ill., Ph.d. Thesis (1971).

2. N. W. Jalufka, R. J. DeYoung, F. Hohl and M. D. Williams, Appl. Phys. Lett. 29, 188 (1976).

3. R. J. DeYoung, N. W. Jalufka, M. D. Williams and F. Hohl, Proc. of Partially Ion.Plasmas - Third Sym. on Uranium Plasmas, Princeton, NJ, June 1976.

4. R. J. DeYoung, N. W. Jalufka, and F. Hohl, Appl. Phys. Lett. 30, 19 (1977).

5. Yuch-Jaw Shin, M. A. Biondi and D. P. Sipler, Phys. Rev. A, 15, 494 (1977).

6. R. J. DeYoung, P. A. Winters, "Power Deposition in He from the Volumetric $^{3}He(n,p)^{3}H$ Reaction," J. of Appl. Phys., Aug. (1977).

7. J. W. Wilson, R. J. DeYoung, "Power Deposition in Volumetric $^{235}UF_6$-He Fission-Pumped Nuclear Lasers," Submitted to J. of Appl. Physics (1977).

8. J. W. Wilson, R. J. DeYoung, "Power Density in Direct Nuclear Pumped ^{3}He Lasers," submitted to J. of Appl. Phys. (1977).

List of Current Publications

1. R. J. DeYoung; N. W. Jalufka, M. D. Williams, and F. Hohl, "Direct Nuclear Pumped Lasers Using the Volumetric ^{3}He Reaction," Proc. of Partially Ionized Plasmas - Third Symposium on Uranium Plasmas, Princeton, N.J., June 1976.
2. N. W. Jalufka, R. J. DeYoung, F. Hohl, and M. D. Williams, "A Nuclear Pumped ^{3}He-Ar Laser Excited by the ^{3}He(n,p)^{3}H Reaction," Appl. Phys. Ltrs., 29, 188 (1976).
3. R. J. DeYoung, N. W. Jalufka, and F. Hohl, "Nuclear-Pumped Lasing of ^{3}He-Xe and ^{3}He-Kr," Appl. Phys. Ltrs., 30, 19 (1977).
4. R. J. DeYoung and P. A. Winters, "Power Deposition in He from the Volumetric ^{3}He(n,p)^{3}H Reaction," J. of Appl. Phys., Aug. 1977.
5. J. W. Wilson and R. J. DeYoung, "Power Density in Direct Nuclear Pumped ^{3}He Lasers," submitted to J. of Appl. Phys., 1977.
6. J. W. Wilson and R. J. DeYoung, "Power Deposition in Volumetric $^{235}UF_6$-He Fission-Pumped Nuclear Lasers," submitted to J. of Appl. Phys. 1977.

List of Conference Presentations

1. R. J. DeYoung, N. W. Jalufka, and F. Hohl, "Direct Nuclear Pumping of ^{3}He-Kr and ^{3}He-Xe," 29th An. Gaseous Electronic Conf., Papers CA8, CA7, CA6, Cleveland, Ohio, October 1976.
2. R. J. DeYoung, N. W. Jalufka, and F. Hohl, "Volumetric Nuclear Pumped Lasers," 1977 IEEE Conf. on Plasma Science, Troy, NY, May 1977.

List of Seminars

1. "Direct Nuclear Pumped Lasers," Vanderbilt Univ., Nashville, TN, 1975.
2. "Direct Nuclear Pumped Laser Research at NASA Langley," University of Paris-Orsay, Orsay, France, August 1976.
3. "Direct Nuclear Pumped Lasers," Miami Univ., Miami, OH, 1977.

FINAL DISCLOSURE OF INVENTIONS REPORT

The following invention report has been made under this grant.

Invention: Direct Nuclear Pumped Lasers using the $^{3}He\ (n,p)\ ^{3}H$ Reaction

NASA Case Number: LAR-12183-1

Date Submitted: January 1977

A patent application on this invention has been made by N. W. Jalufka, F. Hohl, and M. D. Williams of NASA-Langley Research Center and R. J. DeYoung of Vanderbilt University.

NASA DISTRIBUTION LIST FOR FINAL REPORT

(NASA GRANT NSG 1232)

ADDRESSEE:	NO. OF COPIES:
National Aeronautics and Space Administration Langley Research Center Hampton, VA 23665	
ATTN: Dr. F. Hohl, Technical Officer Mail Stop 160	3
Mr. F. S. Kawalkiewicz, Grants Office Mail Stop 126	1
Mr. John Samos, Officer of Technology Utilization and Applications Programs Mail Stop 139A	1
National Aeronautics and Space Administration Division of Research Washington, DC 20546	
ATTN: Mr. F. C. Schwenk, Director	1
Dr. Karlheinz Thom	1
NASA Scientific and Technical Information Facility P.O. Box 8757 Baltimore and Washington Int. Airport, MA 21240	2 (original)
Department of Physics and Astronomy Mr. D. Shepard Vanderbilt University Nashville, TN 37203	5
Office of Sponsored Research Kirkland Hall Vanderbilt University Nashville, TN 37203	1